AAS 08-XXX

OPTICAL NAVIGATION FOR THE ORION VEHICLE

Joel Getchius[*], Dr. Christopher D'Souza[†], and Dr. Timothy Crain

The Orion vehicle is being designed to provide nominal crew transport to the lunar transportation stack in low Earth orbit, crew abort prior during transit to the moon, and crew return to Earth once lunar orbit is achieved. One of the design requirements levied on the Orion vehicle is the ability to return to the vehicle and crew to Earth in the case of loss of communications and command with the Mission Control Center. Central to fulfilling this requirement, is the ability of Orion to navigate autonomously. In low-Earth orbit, this may be solved with the use of GPS, but in cis-lunar and lunar orbit this requires optical navigation. This paper documents the preliminary analyses performed by members of the Orion Orbit GN&C System team.

INTRODUCTION

The Orion vehicle is being designed to provide nominal crew transport to the lunar transportation stack in low Earth orbit, crew abort prior during transit to the moon, and crew return to Earth once lunar orbit is achieved. One of the design requirements levied on the Orion vehicle is the ability to return to the vehicle and crew to Earth in the case of loss of communications and command with the Mission Control Center. Central to fulfilling this requirement, is the ability of Orion to navigate autonomously. In low-Earth orbit, this may be solved with the use of GPS, but in cis-lunar and lunar orbit this requires optical navigation. This paper documents the preliminary analyses performed by members of the Orion Orbit GN&C System team investigating the optical navigation.

The ability of Orion to autonomously navigate without support from the ground is more essential when the loss of communication and command with the ground is coupled with a mission abort scenario. For the mission phases starting at Orion launch and until Orion reaches an altitude equivalent to the GPS shell, it is assumed that autonomous navigation can be sufficiently conducted utilizing an IMU, star tracker, and GPS unit – all of which are baselined in the Orion design. As this sensor suite is a part of the nominal operations concept for entry, descent, and landing phase and has significant historical precedent in other programs (DoD, NASA, ESA, etc.), it is a reasonable assumption that such a sensor suite is feasible for autonomous Orion navigation. Therefore, this navigation concept is not discussed in this paper.

For the flight phases occurring in altitudes above the GPS shell, preliminary feasibility studies determined that without significant changes to the Orion design, attempting to navigate with GPS (via tracking from GPS backside bleed or side lobes) in this region will result in significant periods of less than four satellite tracking. Therefore, the only option would be limited periods of

[*] Title, department, affiliation, address.
[†] Title, department, affiliation, address.

filtering pseudo range measurements from one or two satellites. From a safety and reliability standpoint, this would be undesirable and other, more robust, methods of autonomous navigation have to be examined.

A more feasible option for these flight phases is optical navigation. For the Earth-outbound and Earth-return trajectories, this consists of celestial navigation. That is, navigating via the position of celestial objects such as planets and stars. Specifically, the measurements examined to date have been apparent planetary angular diameter, time of star occultation by a planetary body, and star elevation from a planetary body. The formulation for each of these measurements is reviewed, as well as the feasibility studies conducted to date. In addition, a review of the expected error sources for these measurements is conducted in this paper.

For the flight phase in lunar orbit, often Orion will be oriented such that the star trackers have line of site with the lunar surface only. In this scenario, lunar surface feature tracking (that is crater tracker) is the optical navigation concept of choice. This paper reviews some of the Orion GN&C preliminary lunar surface feature tracking analyses conducted to date as well as reviews issues in formulating these measurements with a star tracker instrument and examines significant error sources.

The results of the feasibility studies are then summarized. Conclusions are extracted that point the Orion GN&C engineers to the belief that optical navigation may be utilized as a method of satisfying the requirement of autonomous navigation. Finally, a quick look at processing issues and algorithm formulation is conducted. Note that the star trackers are not co-located, i.e., one is located on the other-side of Orion. For each of the sensors it is assumed they provide an angular measurement of 0.19 milli-radians 3σ.

VEHICLE CONFIGURATION ASSUMPTIONS

Consider the Orion body axis coordinate frame illustrated in Figure 1.

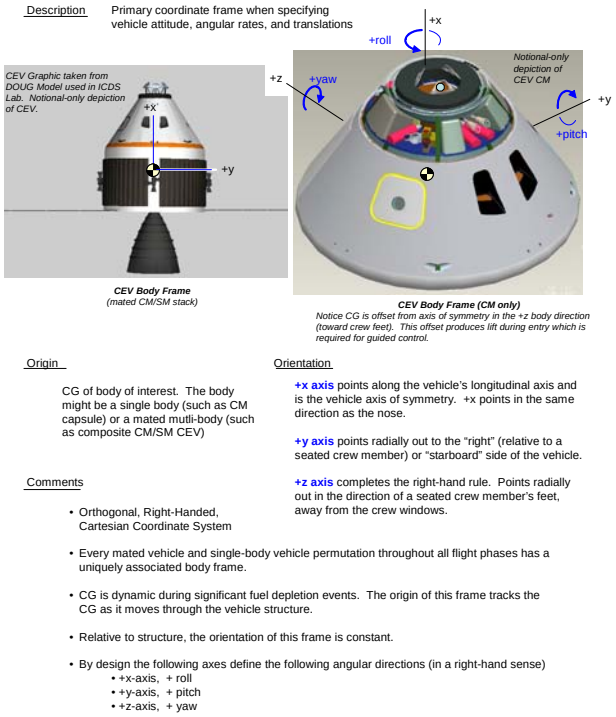

Figure 1: Orion Body Axis Coordinate System (Ref Gonzalez)

Baselined in the Orion design are three optical sensors: two star trackers and one vision navigation sensor (VNS). Both of the star trackers and the VNS are specified to provide image data for processing on the Orion computers. This image processing capability can be utilized to formulate optical navigation measurements from either the measured locations of celestial objects or the measured locations of lunar landmarks. These measurements may then be processed in a navigation filter to obtain an inertial state estimate. While the VNS is slated to be used for relative navigation, there may yet exist the possibility of utilizing this instrument for inertial optical navigation. Ref. Hanak has demonstrated the feasibility of imaging with star trackers.

As the vendor for these instruments has yet to be selected, many of the performance specifications of the instrumentation are an unknown. Therefore, assumptions on the performance for these sensors have to be made. Unless otherwise specified, the VNS is assumed to be mounted boresite along the Orion +X body axis with a field of view of $40° \times 40°$. The two star trackers are mounted in the Orion body X-Y plane but the boresite is canted 57.5° away from the body X axis. The star trackers have a reduced field of view ($18° \times 18°$).

STDN SIMULATION

The simulation tool utilized in the runs described in this paper is the Spacecraft Tracking and Data Network (STDN) simulation. The following description of the STDN tool was taken from Ref Getchius.

Environment Models

Initially, the environment state is randomly perturbed based on the initial environment covariance assigned. This perturbation is calculated via a Gaussian random number generator and the square root of the covariance diagonals. The initial environment covariance was based on

a 500 feet one-sigma position uncertainty and a 1 ft/s one-sigma velocity uncertainty in each inertial axis. The state perturbation was performed completely in inertial coordinates; i.e. no correlations are assigned.

The environment state in the STDN simulation tool is advanced via a fixed time step Encke-Nystrom integrator. The perturbations include gravitational accelerations from the Sun, Moon, and Earth. An additional acceleration term modeled as an exponentially time correlated random variable (ECRV) is also included in the integration of the environment state. The time constant on the ECRV is 40000 seconds with a 1σ approximately 2 μg's each UVW axis.

Sensor Models

Location of the sensors along with field of view and measurement noise have already been discussed in the "Vehicle Configuration Assumptions" section. Additionally, the measurement data rate is assumed to be 10 seconds and all measurements are assumed to be unbiased. Specific measurements generated are phase dependent and will be described in later.

Navigation Models

The initial navigation state was the initial environment state perturbed via a dispersion covariance. This dispersion covariance was based on a 5 km one-sigma position uncertainty and a 5 m/s one-sigma velocity uncertainty in each inertial axis. The off-diagonal elements were initialized to zero.

Like the environment, the navigation algorithms advanced the state with a fixed step Encke-Nystrom integrator. Once again, the perturbations were gravitational accelerations from the Sun, Earth, Moon, and the navigation estimate of the unmodeled acceleration.

The navigation filter algorithm utilized in this study, is the linearized Kalman filter. The filter is a scalar filter and the covariance update equation had been augmented to account for suboptimal filter design. The covariance was propagated in time via the state transition matrix, which was calculated by integrating the time derivative of the state transition matrix. Note that the initial covariance utilized was a lost in space inertial covariance with a 1σ of 1000 km in each position axis and a 1σ of 10 km/s each velocity axis.

The linearized Kalman filter was designed to solve for six inertial state components. Additionally, the navigation state included three inertial unmodeled acceleration values. The unmodeled accelerations in the navigation state were modeled as ECRVs with a time constant of 40000 seconds. Periodically, the reference state was "rectified" with the filtered computed deviation from the reference state. At such rectification points, the filtered computed deviation is zeroed out. The rectification occurred once every hour to maintain the linearization assumption of the navigation filter.

LUNAR OUTBOUDN AND EARTH RETURN NAVIGATION

Orion return to Earth (and outbound to the Moon) will occur on a trajectory with a 3 to 4 day transfer time. During this mission phase, the orientation of Orion with respect to the Sun is important for thermal constraints and power (Orion will carry 2 solar arrays that are normally boresited along the X body axis). Therefore, the baseline attitude is that the Orion vehicle is oriented such the –X body axis is boresited to the Sun. As of now, no barbeque roll is baselined. A barbeque roll, such as the one performed during the Apollo program, consists of the vehicle rolling about an axis such that the Sun will evenly thermally condition the vehicle.

Measurement Models

To date, two types of measurements have been studied for this mission phase: apparent planetary diameter and star elevation from a planetary horizon. These measurements are illustrated in Figure 2.

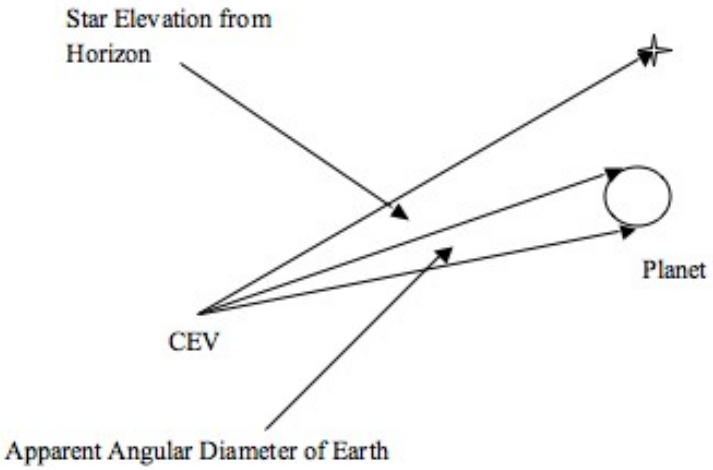

Figure 2: Apparent planetary diameter and star elevation from horizon measurements

Mathematically, the apparent planetary diameter (γ) and the star elevation from planet horizon (λ) can be formulated per Eq. (1) and Eq. (2).

$$\gamma = 2\sin^{-1}\left(\frac{R_{body}}{d}\right) \tag{1}$$

$$\lambda = \cos^{-1}\left(\bar{i}_{Star} \cdot \frac{\bar{d}}{d}\right) - \frac{\gamma}{2} \tag{2}$$

The measurement partials for these equations are shown in Eq. (3) and Eq. (4).

$$H = \frac{\partial \gamma}{\partial \bar{x}_{Body2CEV}} = \frac{-R_{body} 2\bar{x}_{Body2CEV}}{d^3 \sqrt{1-\left(\frac{R_{body}}{d}\right)^2}} \tag{3}$$

$$\frac{\partial\lambda}{\partial\bar{x}_{Body2CEV}} = \frac{-1}{\sqrt{1-\left(\bar{i}_{Star}\cdot\frac{\bar{d}}{d}\right)^2}}\left(\left(\bar{i}_{Star}\cdot\bar{d}\right)\frac{-\bar{x}_{Body2CEV}}{d^3}-\frac{\bar{i}_{Star}}{d}\right)-\frac{1}{2}\frac{-R_{body}2\bar{x}_{Body2CEV}}{d^3\sqrt{1-\left(\frac{R_{body}}{d}\right)^2}}$$

$$H = \frac{\partial\lambda}{\partial\bar{x}_{Body2CEV}} = \frac{-1}{\sqrt{1-\left(\bar{i}_{Star}\cdot\frac{\bar{d}}{d}\right)^2}}\left(\left(\bar{i}_{Star}\cdot\bar{d}\right)\frac{-\bar{x}_{Body2CEV}}{d^3}-\frac{\bar{i}_{Star}}{d}\right)+\frac{R_{body}\bar{x}_{Body2CEV}}{d^3\sqrt{1-\left(\frac{R_{body}}{d}\right)^2}} \quad (4)$$

Note that Eq. 3 and Eq. 4 are for the position components of the state only. The measurement partial with respect to the velocity components of the state is zero. However, for star elevation from the planetary horizon measurements, stellar aberration will shift the observed position of the star based on the velocity of Orion. The shifted position of the star due to stellar aberration is mathematically expressed in Eq. 5.

$$\bar{i}_S^* = unit\left(\bar{i}_S+\frac{\bar{v}_{PV}+\bar{v}_{SE}}{c}\right) \quad (5)$$

The position of the planetary horizon can also be shifted by a similar formulation. Clearly, this formulation will now yield a non-zero measurement partial with respect to the velocity components of the state. Therefore, more state observability has been achieved.

Note that both of the measurements $1/d^3$ term in their measurement partials. This would indicated that the observability of these measurements falls off as Orion moves away from the planetary body. However, both of these measurements have a dependency on the ability to determine the radius of the planetary body. For planetary objects with no atmosphere (such as the moon), the uncertainty in this parameter is driven by terrain. For example, if the star elevation measurement is computed from the bottom of a crater, it will be a different measurement than if it is computed from the top of a mountain. Per Ref. TBD, the terrain of the Moon can vary by ±9 km. Figure 3 plots the uncertainty in the star elevation measurement for various lunar terrain uncertainties as a function of orbital altitude.

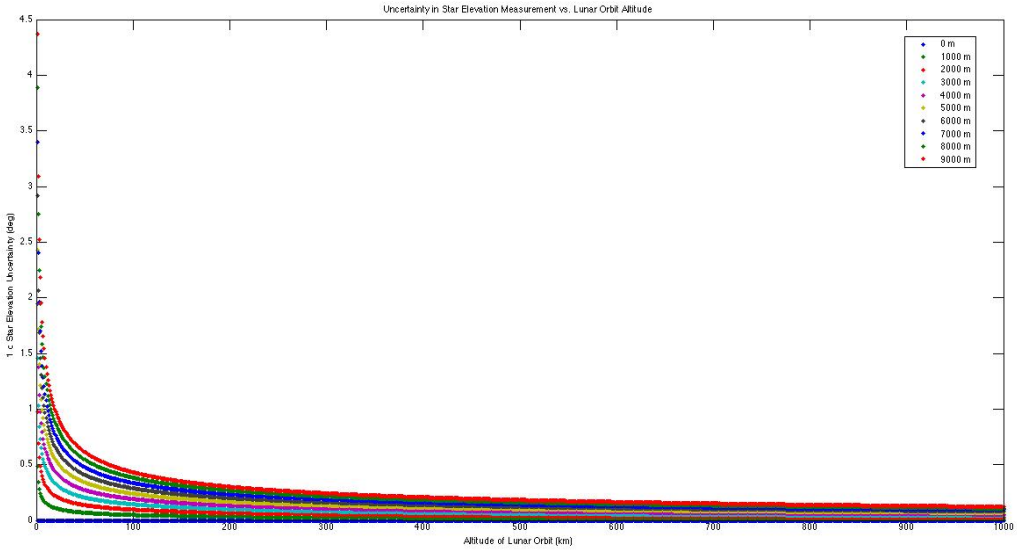

Figure 3: Star elevation from the planetary horizon errors due to uncertainty in lunar radius.

Clearly, there is a conflict between the increased measurement observability from the measurement partial matrix and the increasing measurement uncertainty as Orion approaches a planetary body.

Finally, Ref Battin showed that for the star elevation from planetary horizon measurement, the optimal measurement occurs when the star is 90° from the planetary horizon. Field of view constraints on most sensors will prohibit this type of measurement from being generated. However, it may be possible to generate this 90° from two sensors concurrently. However, such a measurement will induce not only an attitude knowledge dependency, but also sensor mis-alignment issues. Additionally, care might need to be taken so that the sensors produce measurements that are time homogenous and therefore require more active vehicle maintenance of the sensors. For this paper, measurements generated via one sensor are only considered. However, it may be worth while to investigate the potential for generating this measurement with two sensors in the future.

Analysis

Ref Crain et al demonstrated that it is feasible to correct the state utilizing an extended Kalman filter. This preliminary study utilized two star elevation measurements and one apparent planetary diameter measurement for a lunar outbound mission. No field of view checks were performed and no stellar aberration was considered. A limited star catalogue (10 stars) was utilized and the two star elevation measurements were selected so that the first star elevation measurement was as close to 90° as possible and the second measurement was a close to 0°. While limited in scope, this study did demonstrate the feasibility of correcting a navigation state via celestial measurement processing. Therefore, celestial navigation became the baseline navigation design for autonomous navigation for lunar outbound and Earth return trajectories.

Utilizing the STDN simulation a re-examination of celestial navigation performance was done for an Earth return trajectory. First, the nominal attitude provides for some opportunities to

perform celestial navigation. Performing celestial navigation in this attitude is highly desireable in order to minimize the corruption of the navigation state from perturbations from an attitude maneuver. Note that the STDN contains the high fidelity field of view and measurement models described in the "Measurement Models" section that were not contained in the preliminary feasibility study.

For a nominal sortie mission to the moon (approximately seven day on the lunar surface), the Earth return trajectory was run through the STDN simulation and all available measurements were processed with the linearized Kalman filter. Figure 4 illustrates that the VNS consistently tracks Mars, while the star trackers struggled to find available planets.

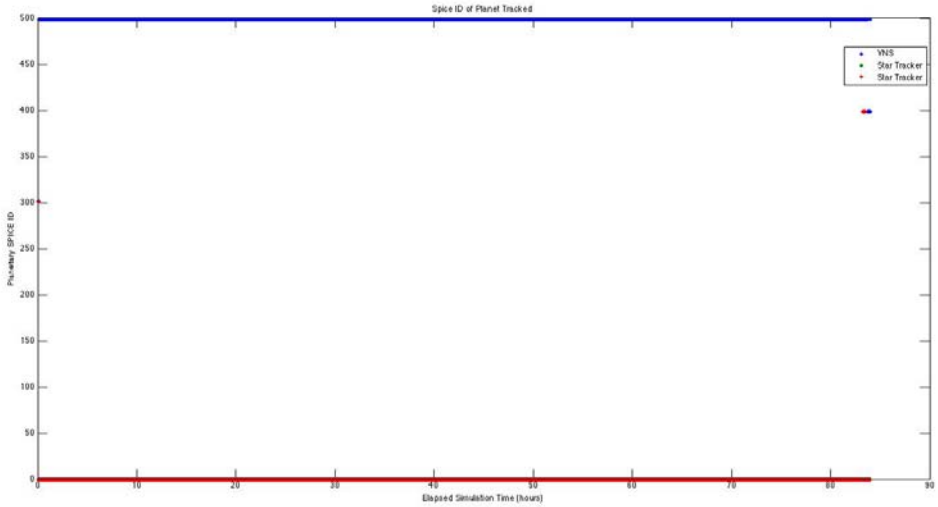

Figure 4: Planetary SPICE ID's for tracked planets.

Due to the large field of view of the VNS, the instrument is capable of seeing a large number of stars. Therefore, a large number of star elevation from planetary horizon measurements may be constructed. Figure 5 plots the number of measurements generated for each camera.

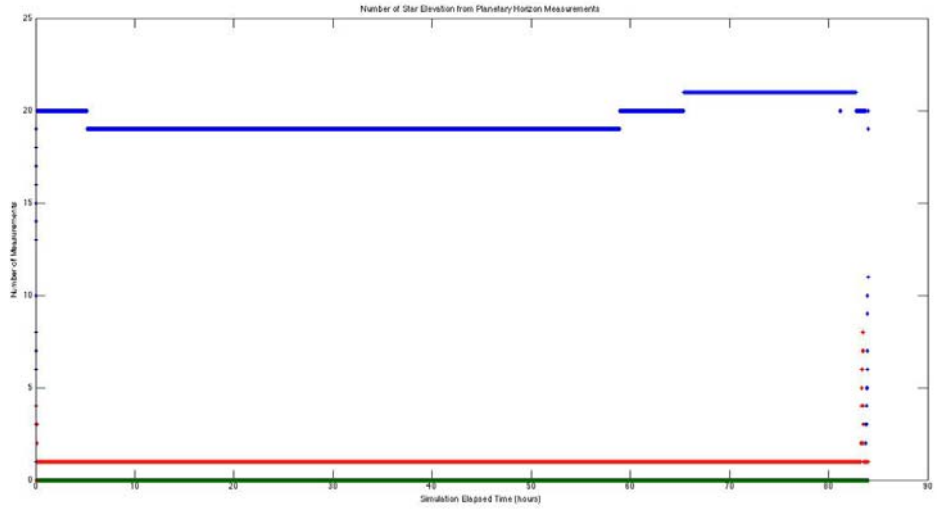

Figure 5: Number of star elevation from planetary measurements for each sensor.

For the Earth return flight phase, the ability to resolve the entry flight path angle is of particular interest. It is estimated that for a safe crew and vehicle return, the flight path angle knowledge will need to be within 0.1°. Figure 6 plots the navigation estimation of the entry flight path angle. Note that no apparent planetary diameter measurements were processed for this run.

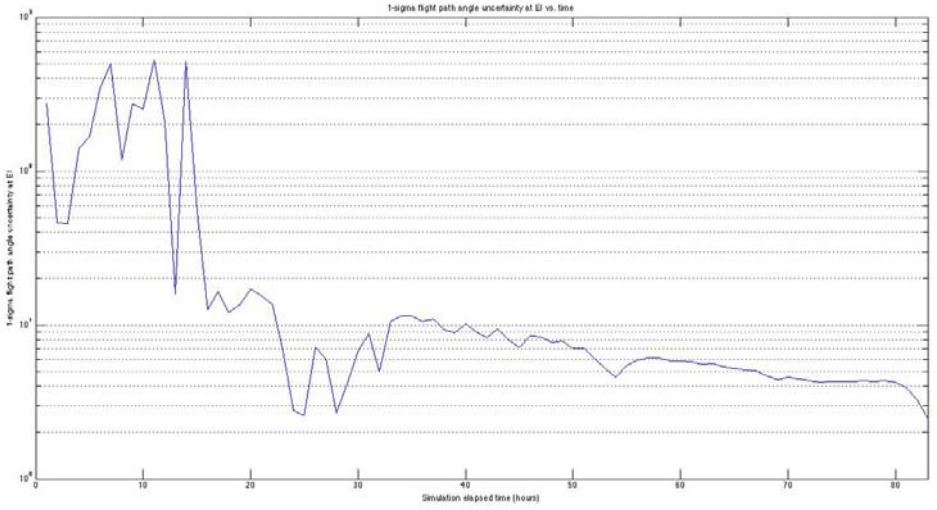

Figure 6: 1σ Flight Path Angle uncertainty vs. time for sun track attitude

Note that it appears that processing star elevation measurements from Mars would be insufficient for providing flight path angle uncertainties less than 0.1°. This is not surprising considering the weak observability of this measurement due to the large distance from Orion to Mars. Therefore, to achieve an adequate navigation solution, it appears that an attitude maneuver will be required in order to track either the Earth or the Moon. Irregardless of the above navigation performance, this may be necessary as trajectory changes for different missions might not provide planets of opportunity to perform celestial navigation.

Therefore, the same Earth return trajectory was re-analyzed in the STDN simulation twice more with Orion +X body axis pointing at the Earth and then again with Orion +X body pointing axis pointing at the Moon. Figure 7 shows the planets being tracked for each sensor in the Earth pointing run and Figure 8 shows the number of star horizon measurements generated for the Earth tracking case. Note for the Earth return case, the apparent planetary diameter of the Earth measurement was available and was processed.

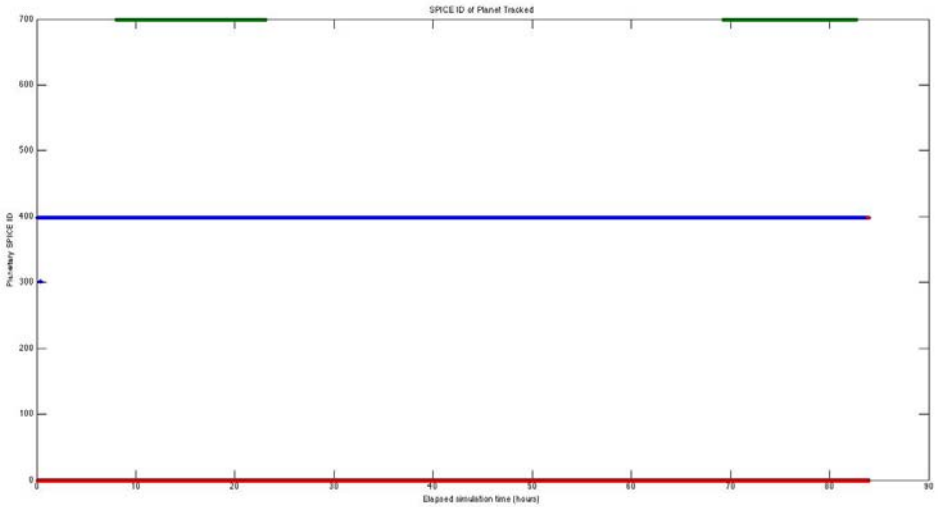

Figure 7: Planetary SPICE ID's for tracked planets

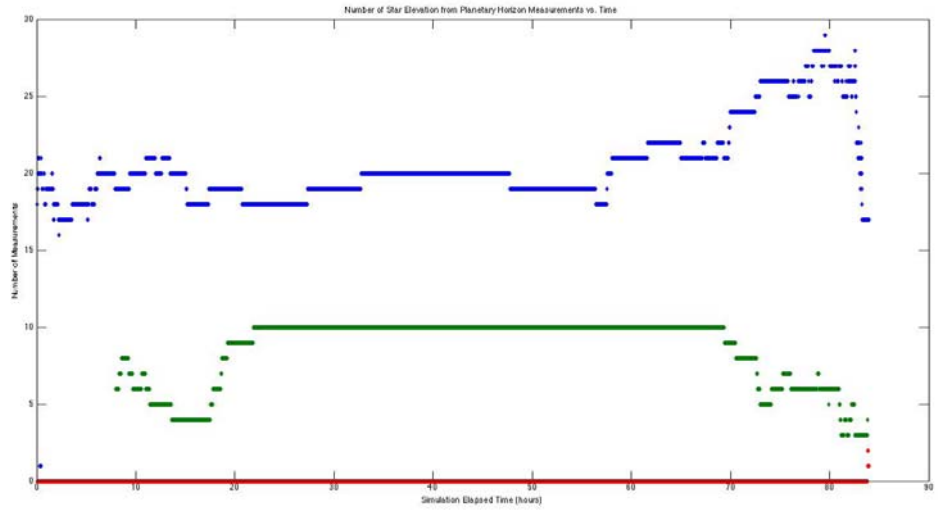

Figure 8: Number of star elevation from planetary measurements for each sensor

For the Moon tracking case, Figure 9 shows the planets being tracked for each sensor and Figure 10 shows the number of star horizon measurements generated. As in the Earth tracking case, the apparent planetary diameter of the Moon measurement was available and processed.

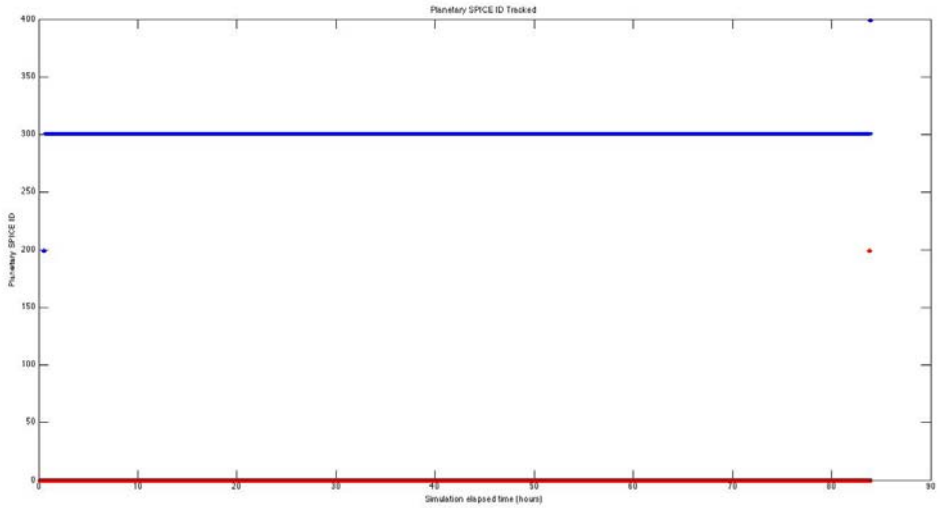

Figure 9: Planetary SPICE ID's for tracked planets

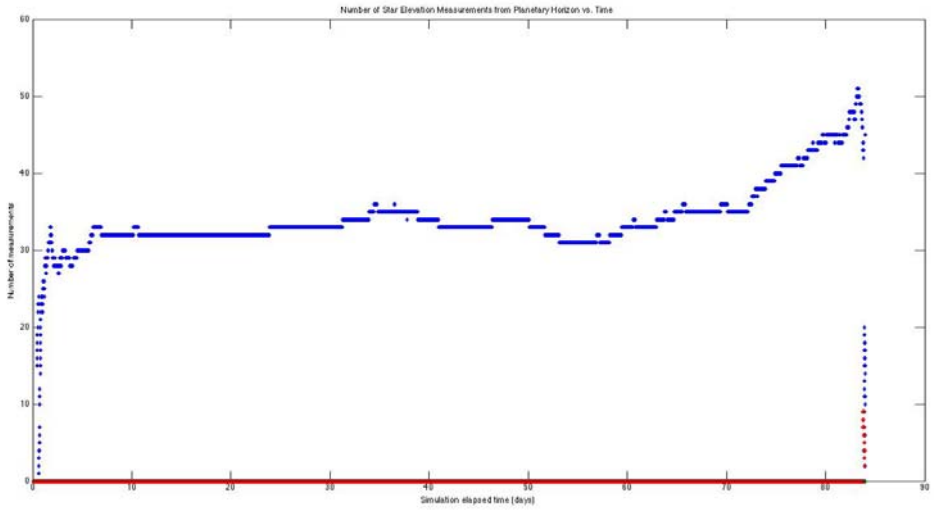

Figure 10: Number of star elevation from planetary measurements for each sensor

For comparison, the navigation 1σ uncertainty of flight path angle at EI for both the Earth tracking and Moon tracking runs is plotted in Figure 11.

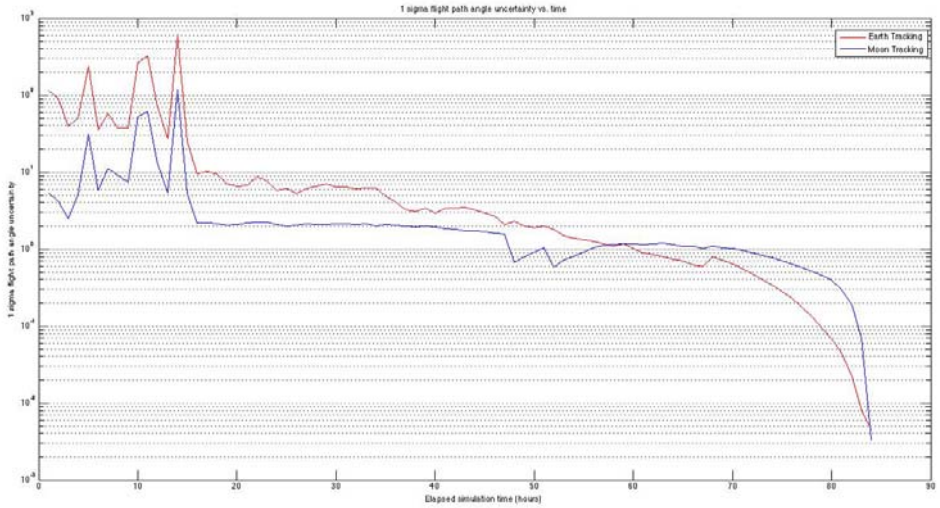

Figure 11: 1σ Flight Path Angle uncertainty vs. time for Earth and Moon track attitude

Note how initially the flight path angle uncertainty is significantly better for the Moon tracking case than for the Earth tracking case. At certain points, this improvement is over an order of magnitude in the uncertainty. However, as the Orion trajectory approaches the Earth, the navigation filter in the Earth tracking case begins to more rapidly improve its knowledge of the flight path angle. At around 60 hours, the Earth tracking case has an entry flight path angle uncertainty less than that of the Moon tracking case.

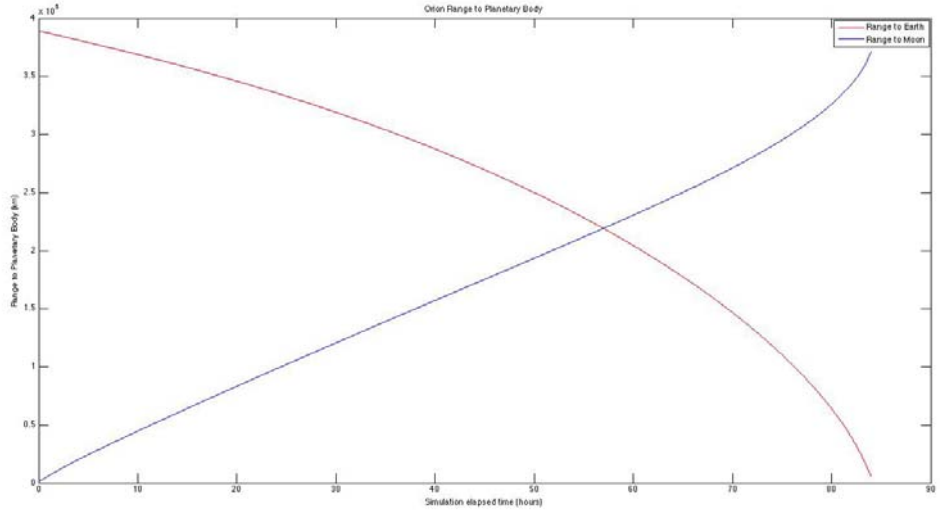

Figure 12: Orion Range to Planetary Body

Figure 12 shows that around the 60 hour mark, the Orion vehicle crosses the geometric center point between the Moon and Earth. That is prior to 60 hours, the Orion was closer to the Moon than the Earth, and post 60 hours it is closer to the Earth than the Moon. It appears that this demonstrates that to maximize the navigation performance from celestial observations, one

should utilize the planetary body closest to the spacecraft. This is consistent with observation of $1/d^3$ in the measurement partials for the two measurements. Encouragingly, it also appears that the increase measurement noise as Orion approaches a planetary body does not inhibit the ability to meet entry flight path angle requirements.

Finally, the ability to image process and generate up to 50 (Figure 10) star elevation from a planetary horizon measurements at rate of once every 10 seconds may not be feasible due to hardware or computational limitations. Additionally, the actual selected sensors may have field of views significantly less than what has been used in this paper. Therefore, a final run of the Moon tracking case was performed, this time limiting each sensor to one star elevation measurement. Figure 13 plots the results of these two runs concurrently.

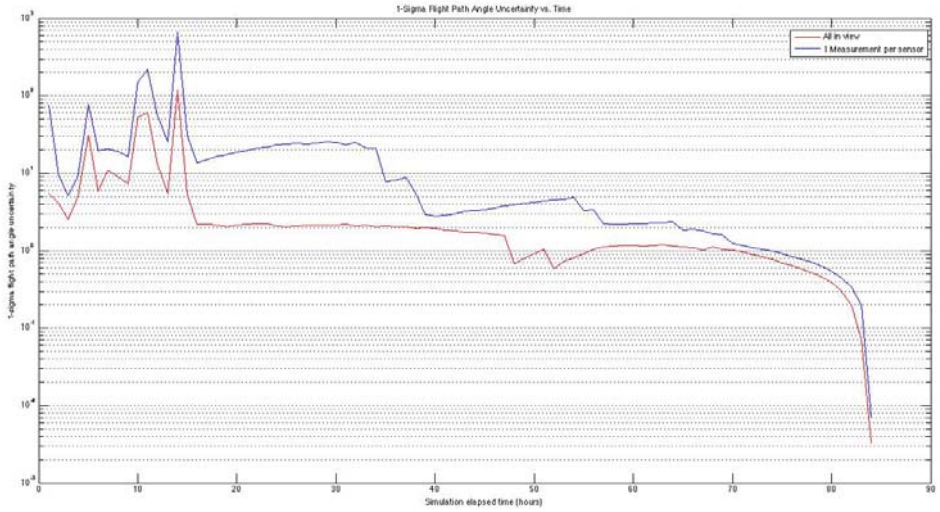

Figure 13: 1-sigma flight path angle uncertainty

As one would expect, there is a decrease in navigation performance due to the reduction of the number of measurements to be processed. However, near a planetary body, this reduction is not terribly significant – at least it is not as significant during the rest of the coasting flight. The reason for this can be illustrated in Figure 14.

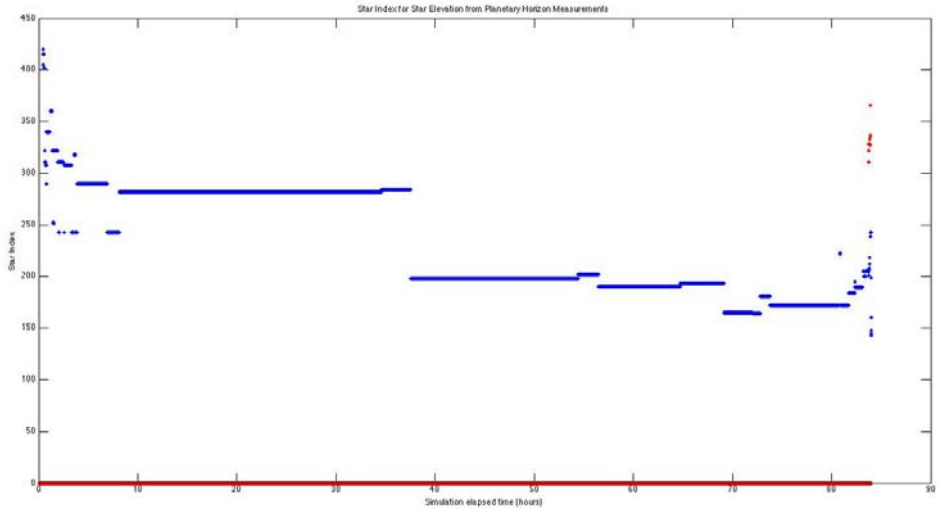

Figure 14: Star index for single star elevation from planetary horizon

Near either the Earth or Moon, there is a rapidly changing trajectory geometry that results in stars quickly dropping in and out of field of view of the sensors. Therefore, even though one star is utilized at time, several stars are utilized over a longer period time resulting in good observeability of the trajectory. Coupled with the stronger correlations in the filter covariance between orbital elements, the impact of fewer measurements at a time is minimized. A future study item could be to re-examine the Sun track attitude hold, this time augmenting the dynamics with a barbeque roll to see if the constant changing measurement field of view improves navigation performance.

LUNAR ORBIT NAVIGATION

The lunar orbit capture maneuver sequence consists of three burns each with the goals of:

1. Capturing Orion into a highly elliptical orbit about the Moon.
2. Changing the plane of the Orion's orbit to ensure access to the desired landing site.
3. Circularizing the orbit of Orion into a 100 km orbit.

The entire sequence may take up to two days to perform and is reversed for the Earth departure sequence. To ensure the ability of the crew to safely and autonomously return to Earth for an abort at anytime in these sequences (or low lunar orbit) navigation via optical measurements of lunar crater locations has been baselined for the Orion vehicle.

Measurement Models

Simplistically, lunar landmark tracking is illustrated in Figure 15.

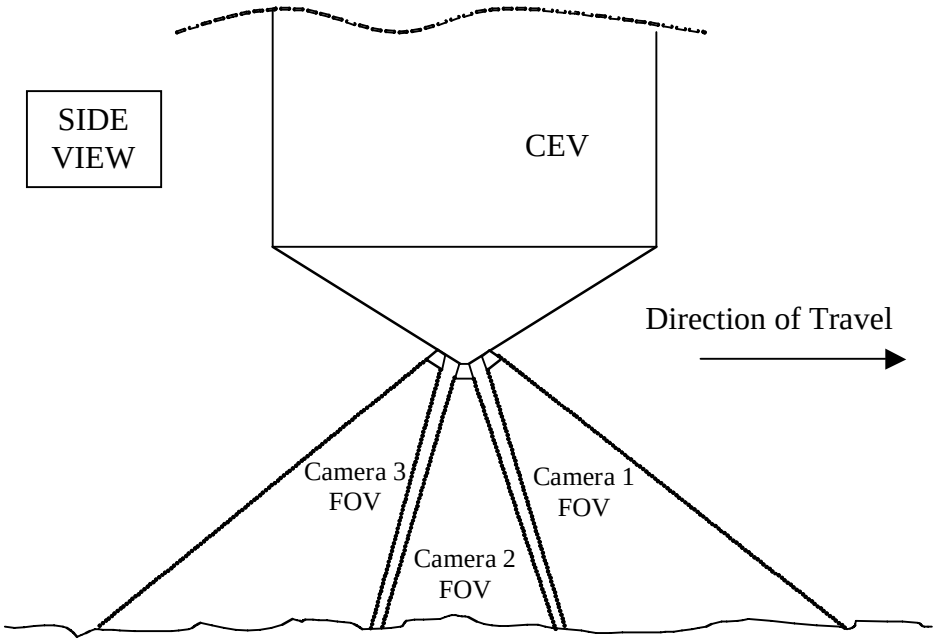

Figure 15: Illustration of Lunar Landmark Tracking

These measurements are simply the observed angular locations of the lunar landmarks by the sensor. Because of the relative proximity of Orion to the lunar landmarks, aberration impacts are minimal and not utilized in measurement generation. Note that in contrast to the work presented on celestial navigation, these measurements have a strong dependency on the accuracy of the attitude state estimation.

Analysis

Crain et al. also performed a feasibility assessment of lunar landmark tracking. Several cases in this study were performed examining the navigation sensitivity to map error, sensor noise, and sensor field of view. Both elliptical and circular trajectories were examined. The tool utilized for these analyses runs is the now defunct LUNA tool developed by Jacobs technology.

The major conclusions reached by this study were:

- Field of view plays a larger roll in the navigation performance than sensor noise. That is, for lunar landmark tracking, it is more beneficial to have a sensor with a larger field of view in order to see more landmarks than it is to have a high accuracy sensor with a smaller field of view.
- Map errors can significantly affect position accuracy, but have little effect on velocity accuracy.

Reference Jacobs has recently impleneted lunar landmark tracking into the official Orion simulation, ANTARES. This work will allow JSC engineers to proceed with analysis and design of lunar landmark tracking navigation with a 6 degree-of-freedom simulation.

CONCLUSION

Orion engineers have performed initial feasibility studies for autonomous navigation in the event of loss of communications with the ground. These studies have led the Orion engineers to baseline utilizing optical navigation for Earth return and lunar outbound mission phases via apparent planetary diameter and star elevation from a planet horizon. For these sets of measurements, much has already been learned. For example, Orion engineers have determined that these measurements are sensitive to trajectory geometries and which planetary body is utilized.

As the Orion design cycle continues, software analysis tools will be improved upon in terms of fidelity. Therefore, Orion engineers may take the opportunity to study several topics related to celestial navigation. Specific items that need to be addressed include navigation algorithm formulation. So far, Kalman filters have been the algorithm utilized. However, other algorithms such as batch least squares or sigma-point filters may be more appropriate.

Once final sensor selection is completed, and exact mounting locations of the sensors is determined, a higher fidelity examination into celestial navigation may be conducted. This includes examining the feasibility of generating these measurements with selected hardware and software interfaces. Additionally, changing operational requirements (ie a barbeque roll) will necessitate additional study. Finally, even though the two measurements described have been baseline, Orion engineers are open to the potential at looking at other measurements available. This includes time of star occultation by a planetary body and the optical tracking of TDRS or GPS satellites.

For lunar orbit, Orion engineers have baselined lunar landmark tracking for autonomous navigation for which similar issues still need to be studied (measurement generation capability and filtering algorithms). Because of the sensitivity to attitude knowledge these types of measurements lend themselves to be studied in a 6 degree of freedom simulation which was recently developed.

ACKNOWLEDGMENT

Any acknowledgments that the author or authors wish to make may appear here.

NOTATION

If mathematical symbols require definition, a table of notation should appear here. A footnote near the beginning of the paper where mathematics is introduced should direct attention of the reader to this table.

REFERENCES

1. Battin,
2. Crain, Timoty et al, “CEV RAC-1 TDS 32: Navigation Without Communication and Autonomous Navigation Assesment,” EG-CEV-06-43, May 2006.
3. Getchius, Joel
4. Jones, Brandon,
5. Gonzalez, Rodolfo, “Coordinate Systems”
6. Hannak, Chad,
7. J. L. Doe and J.W. James, “The Parameterization of Rotation," *Nonlinear Dynamics*, Vol. 32, No. 3, 2005, pp. 71–92.

8. *Style Manual*, American Institute of Physics, 335 East 45th St., New York 17, New York, 2nd Edition, 1959.